Charge and spin interplay in a molecular-dimer-based organic Mott insulator

Natalia Drichko [1,2,*] Shiori Sugiura,[3,4] Minoru Yamashita,[2] Akira Ueda,[2,5] Shinya Uji,[3,4] Nora Hassan,[1] Yoshiya Sunairi,[2] Hatsumi Mori [2] Elena I. Zhilyaeva [6] Svetlana Torunova,[6] and Rimma N. Lyubovskaya[6]

[1]*Institute for Quantum Matter and Department of Physics and Astronomy,*
Johns Hopkins University, Baltimore, Maryland 21218, USA
[2]*The Institute for Solid State Physics, The University of Tokyo, Kashiwa, Chiba 277-8581, Japan*
[3]*National Institute for Materials Science, Tsukuba, Ibaraki 305-0003, Japan*
[4]*Graduate School of Pure and Applied Sciences, University of Tsukuba, Tsukuba, Ibaraki 305-8577, Japan*
[5]*Department of Chemistry, Faculty of Advanced Science and Technology, Kumamoto University, Kumamoto 860-8555, Japan*
[6]*Institute of Problems of Chemical Physics RAS, Chernogolovka, Moscow region, 142432 Russia*

Triangular lattice quasi-two-dimensional Mott insulators based on the bis(ethylenedithio)tetrathiafulvalene (BEDT-TTF) molecule and its analogies present a possibility to produce exotic phases by coupling charge and spin degrees of freedom. In this work we discuss magnetic properties of one such material, κ-(BEDT-TTF)$_2$Hg(SCN)$_2$Cl, which is found at the border of the phase transition between a Mott insulator into a charge ordered state. Our magnetic susceptibility and cantilever magnetization measurements demonstrate how the charge degree of freedom defines magnetic properties for few different charge phases observed in this material as a function of temperature. Between $T_{CO} = 30$ K and $T_S = 24$ K we observe charge and spin separation due to one-dimensional charge stripes formed in this material below $T_{CO} = 30$ K. Below $T_S = 24$ K charge and spin degrees of freedom demonstrate coupling. Spin-singlet correlations develop below 24 K, however, the melting of charge order below 15 K prevents the spin-singlet-state formation, leaving the system in the inhomogeneous state with charge ordered spin-singlet domains and charge and spin fluctuating ones.

I. INTRODUCTION

Recently a lot of research in frustrated magnetism has been focusing on a search for a quantum spin liquid [1,2]. The simplest models of this state consider Heisenberg interactions and magnetic or lattice frustration, where the triangular lattice is the simplest frustrated lattice. The dimensionality of the magnetic system is another parameter defining the behavior of a frustrated system [3]. Additionally, there are theoretical predictions for obtaining these quantum states by coupling spins to other fluctuating degrees of freedom. An example of that are spin-orbital liquids where spins are coupled to fluctuating orbital degrees of freedom [4] or quantum dipole liquids [5–7]. These later states can be realized in organic Mott insulators, where on-site fluctuating electric dipole moments are coupled to the spin degree of freedom [5–7]. Some experimental results suggest a realization of these fluctuating dipole moments and associated with them quantum dipole liquid state [8,9]. Experimental evidence of the coupling of electric dipoles to the spin degree of freedom is necessary to prove that this path to a spin liquid state is at all possible.

Studies of the (BEDT-TTF)$_2$Hg(SCN)$_2$Cl (further named as κ-HgCl, BEDT-TTF stands for -bis(ethylenedithio)tetrathiafulvalene) in the insulating state can provide the answer to this question. This material

is known to form a ferroelectric order of electric dipoles at temperatures between $T_{CO} = 30$ K and 15 K [9–11], which melts on cooling to the lower temperatures. NMR measurements suggest the absence of spin order in this material down to 25 mK [12]. Using SQUID magnetic susceptibility and cantilever torque magnetometery measurements we follow the temperature evolution of magnetic properties in κ-HgCl from metallic into a dipole-ordered state, and further into the melting of the dipole order. We observe the evidence of decoupled charge and spin degrees of freedom below $T_{CO} = 30$ K the temperature of the transition into the charge-ordered state characterized by charge stripes, while below $T_S = 24\,K$ the coupling of charge and spin degrees of freedom defines magnetic properties. No magnetic order is detected in this system down to at least 120 mK, while the exchange interactions are on the order of at least 100 K.

The crystal structure of κ-HgCl, which allows electrical dipole formation on the lattice sites, with $S = 1/2$ associated with each site is shown in Figs. 1 and 3(a). In the layered crystal structure of this material, (BEDT-TTF)$_2^{1+}$ dimers form a triangular lattice in the BEDT-TTF-based layer, with charge $+1e$ and $S = 1/2$ per dimer achieved by a charge transfer between the anion and cation layers. On the charge-order transition, a charge difference of $\Delta n = 0.2e$ between charge-poor and charge-rich molecules of a dimer leads to a dipole solid state [10,11]. This charge distribution is schematically indicated by the red and blue colors in the (BEDT-TTF)$_2$ dimers in Fig. 2. The charge-order transition drives a large

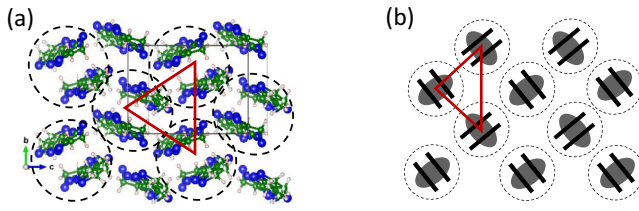*Corresponding author: drichko@jhu.edu

FIG. 1. (a) A projection of the structure of (BEDT-TTF)$_2$ layer of κ-(BEDT-TTF)$_2$Hg(SCN)$_2$Cl on bc crystallographic plane. Dashed line circles indicate dimers of (BEDT-TTF)$_2$. (b) A schematic representation of the 2D layer of (BEDT-TTF)$_2$ dimers. Thick black lines represent BEDT-TTF molecules bound in a dimer by a shared orbital (grey oval). In both (a) and (b) the red triangle shows a unit of triangular lattice.

increase of dc resistivity [10,13] and a notable feature in heat capacity (Fig. 2) [9,11]. While the lattice response is detected on this first-order phase transition [11], no structural phase transition was observed by the x-ray diffraction (XRD) studies so far [10].

On the charge-ordering transition the electronic system changes dimensionality from two-dimensional (2D) to one-dimensional (1D) due to the formation of the charge stripes along the c axis [9–11]. Calculations confirm that the charge order in κ-HgCl results in a high in-plane anisotropy of magnetic exchange interactions J, leading to a suggestion of an effectively 1D magnetism for κ-HgCl [14]. Two scenarios for the ground state of these effectively 1D antiferrmagetic (AF) chains are possible: In the absence of coupling to the lattice, the 1D stripes can evolve into a 1D spin liquid, presenting another possible way to reach a spin liquid state for κ-HgCl [15,16]. A strong coupling of spin degrees of freedom to the lattice can result in a formation of a spin singlet state [17], as observed, for example, in θ-(BEDT-TTF)$_2$RbZn(SCN)$_4$ [18,19].

Melting of the charge order in κ-HgCl below 15 K [9] can lead to the charge disorder and an appearance of domain walls. An interplay of disorder and low-dimensionality is an important direction of research for spin liquid materials. Some materials, a recent example of which is a triangular lattice magnet YbMgGaO$_4$, have the intrinsic structural disorder control of the magnetic ground state [20]. To study structural disorder effects in a controlled fashion, disorder is introduced by x-ray irradiation [21] or doping [22]. κ-HgCl provides a unique situation where charge inhomogeneities are present only in the temperature range below 15 K and their scale is temperature dependent.

Studies of the magnetic properties of κ-HgCl below 50 K in these different charge phases allow us to demonstrate how the charge degree of freedom defines the magnetic properties of the system. Charge order below $T_{CO} = 30$ K resulting in 1D charge stripes leads to a decoupling of charge and spin degrees of freedom in the limited temperature range. Spin singlet correlations in the chains develop at $T_S = 24$ K, however, the long-range spin singlet formation is prevented by the charge-order melting below 15 K. As a result, κ-HgCl shows no long-range magnetic order down to 120 mK and can be understood as an inhomogeneous mix of spin-singlet and spin-fluctuating domains, where the inhomogeneous state
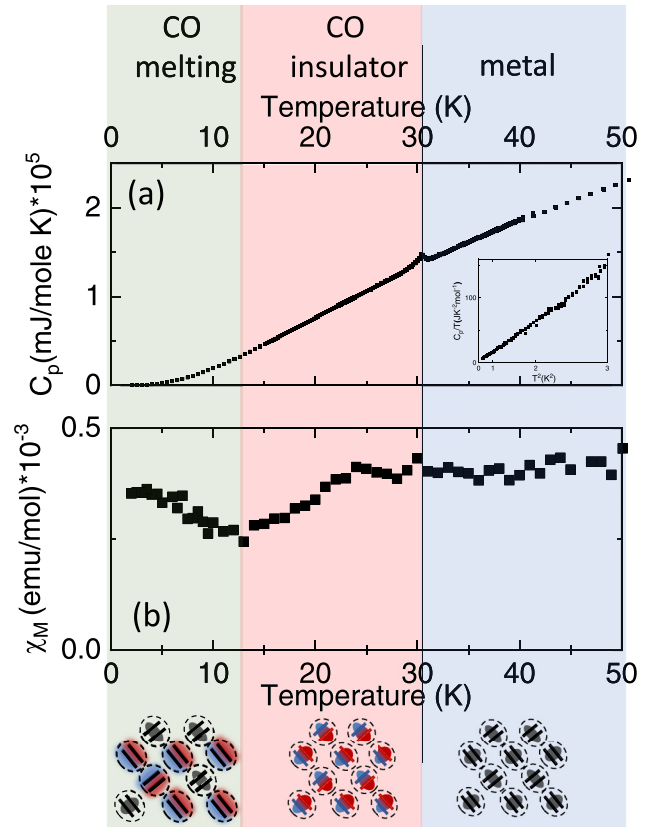

FIG. 2. (a) Temperature dependence of the specific heat C$_p$(T) of κ-(BEDT-TTF)$_2$Hg(SCN)$_2$Cl at 0 T. The inset shows heat capacity in the range 200 mK to 3 K. Note $\gamma = 0$ within the error of the measurements. (b) Temperature dependence of $\chi_M(T)$. Three regimes related to the charge degree of freedom [9] are indicated by color. Schematic charge distribution on the orbital of (BEDT-TTF)$_2$ dimer is shown, where grey indicates homogeneous charge in the metallic state above $T_{CO} = 30$ K, red are the charge-rich, and blue are the charge-poor molecules in the charge-ordered insulating state. Low-temperature mixed state below 15 K consists of components with homogeneous charge distribution and dimers where charge order is preserved as static or slowly fluctuating, as depicted by blurred colors.

is a consequence of the system being close to the phase border with the ferroelectric state [23].

II. EXPERIMENT

Single crystals of κ-(BEDT-TTF)$_2$Hg(SCN)$_2$Cl (κ-HgCl) were prepared by electrochemical oxidation of the BEDT-TTF solution in 1,1,2-trichloroethane (TCE) at a temperature of 40° C and a constant current of 0.5 μA. A solution of Hg(SCN)$_2$, [Me$_4$N]SCNKCl, and dibenzo-18-crown-6 in a 1 : 0.7 : 1 molar ratio in ethanol/TCE was used as supporting electrolyte for the κ-HgCl preparation. The composition of the crystals was verified by electron probe microanalysis and XRD.

The temperature dependence of heat capacity in the temperature range from 50 K to 200 mK was measured using a Quantum Design PPMS system equipped with the DR the option for crystals of the mass of 2 to 4 mg. The temperature dependence of magnetic susceptibility $\chi_M(T)$ of a polycrystal sample of $m = 2.451$ mg was measured using Quantum Design MPMS in field of 1 T in the temperature range from 2 to 300 K. The magnetic torque of single crystals was measured using a magnetic cantilever setup in the temperature range down to 120 mK and magnetic fields up to 18 T. The setup and the details of the data analysis are discussed in [24].

III. RESULTS

On the metal-insulator transition in κ-HgCl at $T_{CO} = 30$ K, heat capacity shows a distinct peak [see Fig. 2(a)]. No other phase transition is detected down to 200 mK (see inset in Fig. 2). The extrapolation down to 0 K suggests a negligible linear component of γ term in heat capacity $C_p = \beta T^3 + \gamma T$.

The magnetic susceptibility $\chi_M(T)$ of a polycrystal sample of 2.451 mg measured at 1 T [Fig. 2(b)] reveals a complex temperature dependence. Above $T_{CO} = 30$ K κ-HgCl shows Pauli susceptibility of about 4×10^{-4} emu/mol. This value is close to that of the other BEDT-TTF-based organic conductors [25]. At the charge-order transition magnetic susceptibility $\chi_M(T)$ does not show any change within the noise of the measurements. Instead, magnetic susceptibility starts to decrease abruptly on cooling below about 24 K.[1] Decreasing susceptibility in the temperature range between 24 K and 15 K can be fit by a magnetic susceptibility of a gapped system $e^{-\frac{\Delta}{k_B T}}$, which yields a gap $\Delta = 36$ K $= 1.5 T_c$ (see the Appendix) with the assumption that susceptibility of a charge ordered system will become $\chi_{CO} = 0$ on cooling. Magnetic susceptibility starts to rise again on cooling the sample below 15 K, and saturates below about 5 K, with the saturation values of about 3.5×10^{-4} emu/mol. No indication of magnetic ordering is found in $\chi_M(T)$ of κ-HgCl down to 2 K.

BEDT-TTF-based crystals are typically very small and posses very low magnetic susceptibility (Fig. 2). To understand the nature of the low-temperature magnetic state, we performed measurements of the cantilever torque magnetization for single crystals of κ-HgCl. This method proved to be the most sensitive to detect magnetic order and was successfully applied to organic Mott insulators [26–28]. The magnetic torque signal measured for κ-HgCl is described well by the following equation:

$$\tau = \tau_0 + \tau_\theta \sin(\theta - \theta_1) + \tau_{2\theta} \sin 2(\theta - \theta_2). \quad (1)$$

In the κ-HgCl torque response, the $\tau_\theta \sin(\theta - \theta_1)$ component does not change with the applied magnetic field at all
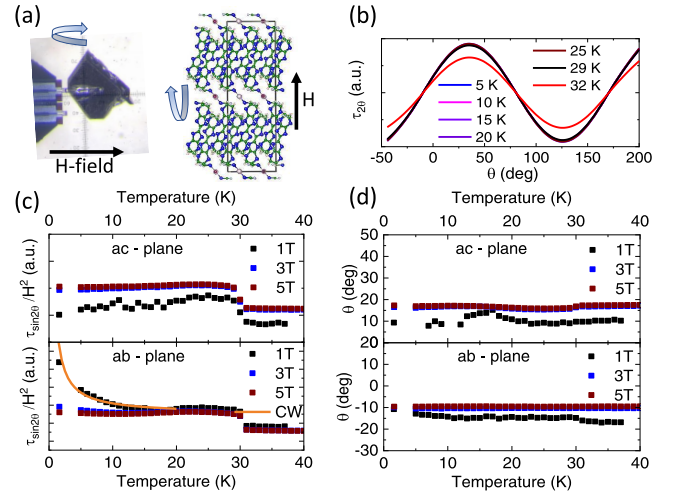

FIG. 3. (a) Scheme of cantilever torque magnetometery experiment with the rotation direction for the *ab* plane shown with blue arrow and magnetic field direction shown in black. (b) Angle dependence of paramagnetic component of torque $\tau_{2\theta}$ at 5 T, rotation in the *ab* plane for temperatures related to the different charge states of κ-(BEDT-TTF)$_2$Hg(SCN)$_2$Cl. (c) Temperature dependence of the paramagnetic torque amplitude $\tau_{2\theta}$ in *ac* plane and *ab* planes. (d) Temperature dependence of the phase θ_2 in the *ac* and *ab* planes.

measured temperatures (see the Appendix). We conclude that it fully corresponds to the gravity force and no ferromagnetic component of torque was detected. The $\tau_{2\theta} \sin[2(\theta - \theta_2)]$ component in the torque response of κ-HgCl corresponds to the paramagnetic response.

Cantilever torque magnetization measurements show the persistence of the paramagnetic response when κ-HgCl is cooled through the charge-order transition at 30 K and below this temperature, but detect an abrupt increase of torque amplitude $\tau_{2\theta}$ at $T_{CO} = 30$ K, as shown in Fig. 3. The torque amplitude $\tau_{2\theta}$ for the rotation in the *ab* plane at 1 T roughly follows the temperature dependence of magnetic susceptibility, with a decrease at about 20 K, and an increase below 15 K. The phase θ_2 for the rotation in the *ac* plane follows this temperature behavior as well, while the amplitude stays constant on cooling. These effects are weak and are suppressed at 3 T.

Magnetization is probed by measuring the torque amplitude dependence on magnetic field H at an angle where the amplitude of the torque is maximum, see Fig. 4. At temperatures $T = 20, 10, 5, 1.9$ K for the field up to $H = 5\,T$ torque, τ shows a parabolic dependence $\tau \propto H^2$, suggesting a purely paramagnetic state. The $\tau \propto H^2$ behavior of magnetization was confirmed at $T = 120$ mK in magnetic field up to 17.5 T (Fig. 4).

IV. DISCUSSION

A picture of an exotic spin and charge behavior in κ-HgCl forms when we put together the results obtained with these different probes. An absence of a change of magnetic susceptibility at $T_{CO} = 30$ K and purely paramagnetic torque response below the transition is unexpected: The character of $\chi_M(T)$ should change from Pauli to a behavior of an insulator with

---

[1]A seemingly similar material κ-ET$_2$Cu$_2$(CN)$_3$ that shows a very close magnetic susceptibility values of $\chi_M = 5*10^{-4}$ emu*mol^{-1} at 30 K [39] is not the right compound to compare to. This system shows magnetic excitations spectrum of a two-dimensional triangular lattice of ET dimers, and lacks any charge disproportionation. In any case, $\chi_M(T)$ of κ-HgCl decreases faster than a triangular lattice $S = 1/2$ magnetic susceptibility [51].
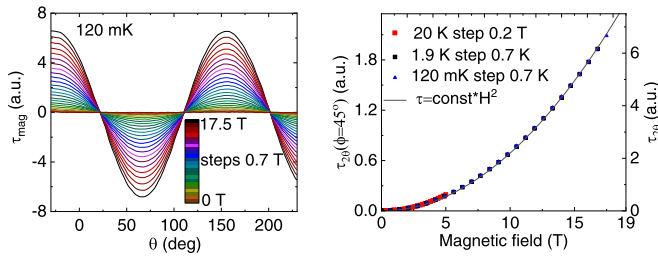
FIG. 4. Magnetization of κ-(BEDT-TTF)$_2$Hg(SCN)$_2$Cl measured my magnetic cantilever torque magnetometery. (a) Magnetic field dependence of torque signal at 120 mK for magnetic field H in the range from 0 to 17.5 T. (b) Field dependence of $\tau_{2\theta}$.

unpaired spins or a spin singlet state. However, the charge-ordering transition only leads to a jump in the paramagnetic component of the torque amplitude $\tau_{2\theta}$ at 30 K, which is a measure of the anisotropy of the g-factor [29] and responds to the change of the electronic structure on the transition.

$\chi_M(T)$ starts to decrease on cooling only below $T_S = 24$ K, suggesting a development of spin singlet correlations. This decrease is in agreements with the previous results of ESR measurements [13]. Heat capacity does not show any indication of a phase transition at 24 K, but it is known to be not a sensitive indicator of a magnetic transition neither in 1D [30] nor in 2D [31] organic-based systems.

The development of a spin singlet state is one of the expected consequences of the charge stripes formation [17]. Striking here is a decoupling of the charge-order transition temperature ($T_{CO} = 30$ K) and the temperature of the spin singlets formation $T_S = 24$ K. It demonstrates the decoupling of charge and spin degrees of freedom in this temperature range as a consequence of 1D electronic structure [9–11] of charge stripes in κ-HgCl. Such a decoupling is common in 1D TMTTF -based materials, which undergo a transition into an antiferromagnetically ordered or spin-Peierls state at temperatures of about ten times lower than the temperature of a metal-insulator transition [32,33]. To the best of our knowledge, it is observed for the first time in a layered system as a result of a dimensional crossover associated with 1D charge stripes formation.

A signature of a singlet state in magnetic torque would be a decrease of torque amplitude $\tau_{2\theta}$ down to zero. We observe that magnetic torque of κ-HgCl preserves its paramagnetic character below 24 K and shows only a slight decrease of the torque amplitude $\tau_{2\theta}$ in the ab plane. A decrease of χ_M without a detectable long-range order suggests that AF order or spin singlet pairs which will posses $\chi_{CO} = 0$ are formed with a certain correlation length in the temperature range between 24 and 15 K, without long-range order. Changes of the phase values of torque in the ac plane observed at 1 T (Fig. 2) follow the susceptibility behavior and are apparently due to orphan spins appearing as a result of short range AF or spin single correlations [34].

At temperatures below 15 K, the charge order starts to melt [9] and magnetic susceptibility increases again. In the resulting inhomogeneous system depicted schematically in Fig. 2 the charge-order melted fraction ρ would provide $\chi_M = \rho \chi_H + \chi_D$, where χ_H corresponds to the response of

the charge melted fraction with finite susceptibility and χ_D is the susceptibility of the domain walls between fractions with χ_H and $\chi_{CO} = 0$. According to our previous results, the charge melted fraction ρ increased on cooling from $\rho = 0$ in the charge-ordered state to $\rho = 1/3$ at 2 K [9]. The increase of both $\rho \chi_H$ and χ_D components on melting of the charge order can add to the increase of the total χ_M of the sample as the temperature is lowered from 15 to 2 K.

The system where charge order is melting is intrinsically inhomogeneous. If paramagnetic spins of inhomogeneities are noninteracting, they would produce a Curie-like response [35]. However, the increase of magnetic susceptibility below 15 K differs from a simple Curie-like response: Instead of diverging as $1/T$, $\chi_M(T)$ shows a weaker temperature dependence and flattens below 5 K. The increase of torque amplitude $\tau_{2\theta}$ is observed only in the ab plane, showing that the system preserved some anisotropy and also deviates from the pure Curie response. We can conclude that paramagnetic spins of the melted charge order and domain walls are interacting, and present a more complicated picture than orphan spins of defects (see Ref. [34] and references therein). Recently is was suggested that two spins on the ends of fluctuating charge-order chains interacting through a non-charge-ordered dimer could interact ferromagnetically [36]. It is worth noting that the increase and saturation of $\chi_M(T)$ below 15 K in κ-HgCl is similar to the dipole liquid candidate κ-(BEDT-TTF)$_2$Hg(SCN)$_2$Br magnetic susceptibility, but on a much smaller scale. Other models developed for quantum paraelectrics also suggested an increase of magnetic susceptibility due to fluctuating electric dipoles [37].

If the increase of the $\chi_M(T)$ on cooling and the temperature dependence of torque at low fields are produced by the interacting domain walls, they become fully polarized already at 3 T according to the torque measurements. This result is in agreement with a suppression of a peak in T^{-1} in NMR response [12] by the magnetic field directed perpendicular to BEDT-TTF-based layers, and suggests that the origin of the peak is the response of the domain walls. According to the Raman data in magnetic field in this direction, the charge distribution itself does not change in field up to 30 T [38].

No indication of magnetic ordering is observed in the magnetic cantilever torque studies of κ-HgCl down to 120 mK. The paramagnetic torque amplitude $\tau_{2\theta} \propto H^2$ up to 17.5 T and the phase is constant with field. This shows the absence of magnetic order or of a spin singlet state in the fraction of the κ-HgCl crystal where charge order is melted and the lattice sites possess one unpaired electron ($S = 1/2$) with estimated magnetic exchange J of the order of 100 K or higher [8,14,36]. This part of the system provides the response suggestive of a spin liquid state from NMR measurements [12].

The low-temperature magnetic state of both charge-ordered and charge-melted fractions in κ-HgCl has signatures very different from the other spin liquid candidates triangular 2D dimer Mott insulators [31,39–43]. In the $S = 1/2$ triangular lattice organic Mott insulators without a charge degree of freedom, such as κ-(BEDT-TTF)$_2$Cu$_2$(CN)$_3$[8,44], κ-(BEDT-TTF)$_2$Ag$_2$(CN)$_3$ [45], and Pd(dmit)$_2$-based materials [46], Raman scattering spectroscopy detects a continuum of magnetic excitations well understood in terms of $S = 1/2$ on a triangular lattice [47–50]. This continuum is absent in the
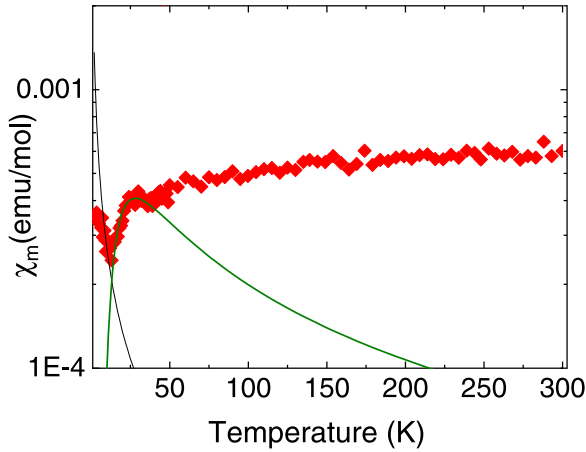
FIG. 5. Magnetic susceptibility of κ-(BEDT-TTF)$_2$Hg(SCN)$_2$Cl polycrystal sample measured by SQUID magnetometer using H=1 T in the temperature range from 300 to 2 K.

Raman scattering spectra of κ-HgCl [8] down to 10 K, and magnetic excitations in this material are still to be detected. In addition, in contrast to dimer Mott insulators without charge order [24,41] κ-HgCl shows a $\gamma = 0$ linear term in the heat capacity [8], suggesting that the magnetic excitations spectrum is gapped, which can be a consequence of a finite size of domains with fluctuating spins. Apparently, the inhomogeneities and domain walls do not produce the low-temperature input in γ.

The key difference between the electronic structure of κ-HgCl and the triangular 2D Mott insulators discussed above is the smaller intradimer integral in κ-HgCl, which results in a weaker dimerization and active charge degree of freedom [9,11,23]. The relevant phase diagram of the κ-phase organics where the intradimer transfer integral serves as a tuning parameter, tuning a system from an antiferromagnetic Mott insulator at high dimerization to a charge-order ferroelectric at low dimerization was theoretically discussed in Ref. [23]. We have already shown that κ-HgCl was found on the border between these two phases and experienced a reentrant charge-order melting transition due to the competition of electronic repulsion, which leads to charge order and antiferrmagnetic interactions [9,23]. The formation of domains at low temperature in this material is a consequence of the competition of these parameters close to the phase border. In this work we demonstrate that the ordered versus fluctuating domains are found not only in the charge sector, but also in the spin degree of freedom.

V. CONCLUSION

In conclusion, our data experimentally demonstrate the importance of the interplay of the charge and spin degrees of freedom for the dimer Mott insulators, previously suggested theoretically [5,23]. We reveal how the charge state in κ-HgCl in each temperature range defines the magnetic properties. On cooling we first observe a spin-charge separation in the narrow temperature range between $T_{CO} = 30$ K and $T_S = 24$ K due to the formation of 1D charge stripes. The effects at lower temperatures demonstrate coupling between charge and spin
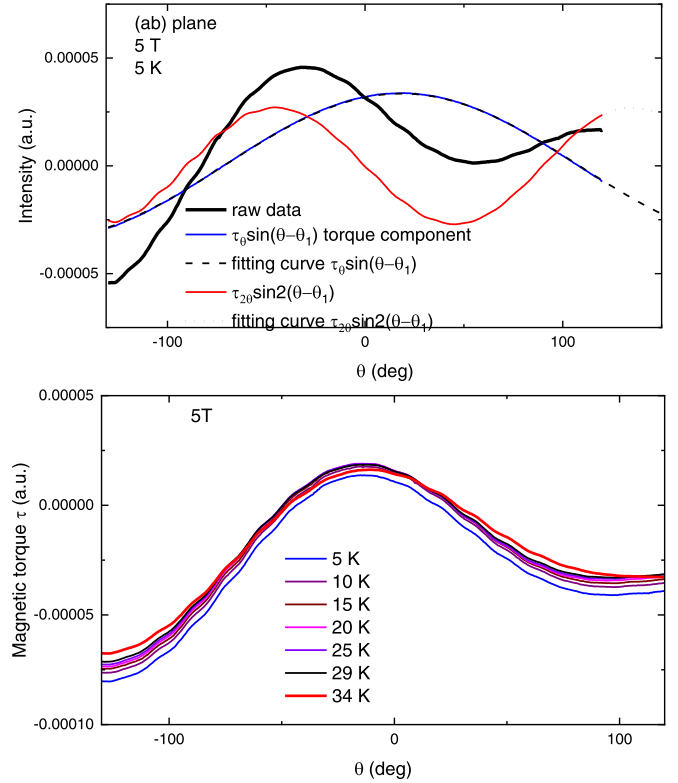

FIG. 6. Upper panel: Cantilever magnetic torque data analysis and example for the data for the rotation in *ab* plane at 5 K in magnetic field of 5 T. The figure shows original data and $\tau_\theta \sin(\theta - \theta_1)$, and $\tau_{2\theta} \sin2(\theta - \theta_1)$ components with the respective fitting curves. Lower panel: Raw data of κ-(BEDT-TTF)$_2$Hg(SCN)$_2$Cl obtained by cantilever magnetic torque measurements. Measurements are done for rotation in *ab* plane, $H = 5$ T. Angle dependence of $\tau_{2\theta}$ extracted from these measurements is presented in Fig. 3(b).

degrees of freedom. Below $T_S = 24$ K, the system shows spin singlet correlations, but preserves considerable paramagnetic torque response, proving that these correlations never develop into a long-range order. Moreover, below 15 K the melting of the charge order prevents the spin singlet formation in the whole system and leads to an inhomogeneous state with spin singlet charge ordered domains and domains which do not show either charge or magnetic order.

APPENDIX

1. Magnetic susceptibility

Figure 5 shows magnetic susceptibility data in the whole measured range. The figure also demonstrates a curve of $\chi_{\text{dimer}} = Ae^{-\frac{\Delta}{k_B T}}$ which can describe $\chi_M(T)$ in the temperature range between 24 and 15 K, and $\chi_{\text{Curie}} = C/T$ to compare to the low-temperature behavior of $\chi_M(T)$.

2. Cantilever magnetic torque measurements

Figure 6 presents an example of analysis of the cantilever magnetic torque data. The full torque τ (black curve) is reproduced well by the sum of $\tau_\theta \sin(\theta - \theta_1)$ and $\tau_{2\theta} \sin 2(\theta - \theta_1)$ components. Calibration of the cantilever response by the gravity signal is discussed in detail in Ref. [24].

[1] L. Savary and L. Balents, Rep. Prog. Phys. **80**, 016502 (2017).

[2] C. Broholm, R. Cava, S. Kivelson, D. Nocera, M. Norman, and T. Senthil, Science **367**, eaay0668 (2020).

[3] H. Diep *et al.*, *Frustrated Spin Systems* (World Scientific, Singapore, 2013).

[4] L. Balents, Nature (London) **464**, 199 (2010).

[5] C. Hotta, Phys. Rev. B **82**, 241104(R) (2010).

[6] M. Naka and S. Ishihara, Phys. Rev. B **93**, 195114 (2016).

[7] N. Y. Yao, M. P. Zaletel, D. M. Stamper-Kurn, and A. Vishwanath, Nat. Phys. **14**, 405 (2018).

[8] N. Hassan, S. Cunningham, M. Mourigal, E. I. Zhilyaeva, S. A. Torunova, R. N. Lyubovskaya, J. A. Schlueter, and N. Drichko, Science **360**, 1101 (2018).

[9] N. M. Hassan, K. Thirunavukkuarasu, Z. Lu, D. Smirnov, E. I. Zhilyaeva, S. Torunova, R. N. Lyubovskaya, and N. Drichko, npj Quantum Mater. **5**, 15 (2020).

[10] N. Drichko, R. Beyer, E. Rose, M. Dressel, J. A. Schlueter, S. A. Turunova, E. I. Zhilyaeva, and R. N. Lyubovskaya, Phys. Rev. B **89**, 075133 (2014).

[11] E. Gati, J. K. H. Fischer, P. Lunkenheimer, D. Zielke, S. Köhler, F. Kolb, H.-A. K. von Nidda, S. M. Winter, H. Schubert, J. A. Schlueter, H. O. Jeschke, R. Valent, and M. Lang, Phys. Rev. Lett. **120**, 247601 (2018).

[12] A. Pustogow, T. Le, H.-H. Wang, Y. Luo, E. Gati, H. Schubert, M. Lang, and S. Brown, Phys. Rev. B **101**, 140401 (2020).

[13] S. Yasin, E. Rose, M. Dumm, N. Drichko, M. Dressel, J. Schlueter, E. Zhilyaeva, S. Torunova, and R. Lyubovskaya, Phys. B: Condens. Matter **407**, 1689 (2012).

[14] A. C. Jacko, E. P. Kenny, and B. J. Powell, Phys. Rev. B **101**, 125110 (2020).

[15] F. Mila, Eur. J. Phys. **21**, 499 (2000).

[16] H. Watanabe and H. Seo, J. Phys. Soc. Jpn. **86**, 033703 (2017).

[17] S. Dayal, R. T. Clay, H. Li, and S. Mazumdar, Phys. Rev. B **83**, 245106 (2011).

[18] H. Mori, S. Tanaka, T. Mori, and A. Fuse, Synth. Met. **86**, 1789 (1997).

[19] K. Kanoda and R. Kato, Annu. Rev. Condens. Matter Phys. **2**, 167 (2011).

[20] I. Kimchi, A. Nahum, and T. Senthil, Phys. Rev. X **8**, 031028 (2018).

[21] T. Furukawa, K. Miyagawa, T. Itou, M. Ito, H. Taniguchi, M. Saito, S. Iguchi, T. Sasaki, and K. Kanoda, Phys. Rev. Lett. **115**, 077001 (2015).

[22] T. Kawamata, N. Takahashi, T. Adachi, T. Noji, K. Kudo, N. Kobayashi, and Y. Koike, J. Phys. Soc. Jpn. **77**, 034607 (2008).

[23] M. Naka and S. Ishihara, J. Phys. Soc. Jpn. **79**, 063707 (2010).

[24] M. Yamashita, N. Nakata, Y. Senshu, M. Nagata, H. M. Yamamoto, R. Kato, T. Shibauchi, and Y. Matsuda, Science **328**, 1246 (2010).

[25] G. Sekretarczyk, A. Graja, and L. Goldenberg, Synth. Met. **24**, 161 (1988).

[26] M. Pinterić, M. Miljak, N. Biškup, O. Milat, I. Aviani, S. Tomić, D. Schweitzer, W. Strunz, and I. Heinen, Eur. Phys. J. B **11**, 217 (1999).

[27] T. Isono, T. Terashima, K. Miyagawa, K. Kanoda, and S. Uji, Nat. Commun. **7**, 13494 (2016).

[28] D. Watanabe, M. Yamashita, S. Tonegawa, Y. Oshima, H. Yamamoto, R. Kato, I. Sheikin, K. Behnia, T. Terashima, S. Uji, *et al.*, Nat. Commun. **3**, 1090 (2012).

[29] S. Uji, J. Brooks, M. Chaparala, S. Takasaki, J. Yamada, and H. Anzai, Phys. Rev. B **55**, 12446 (1997).

[30] M. de Souza, A. Brühl, J. Müller, P. Foury-Leylekian, A. Moradpour, J.-P. Pouget, and M. Lang, Phys. B: Condens. Matter **404**, 494 (2009).

[31] S. Yamashita and Y. Nakazawa, J. Therm. Anal. Calorim. **99**, 153 (2010).

[32] B. Salameh, S. Yasin, M. Dumm, G. Untereiner, L. Montgomery, and M. Dressel, Phys. Rev. B **83**, 205126 (2011).

[33] M. Dressel, Naturwissenschaften **94**, 527 (2007).

[34] K. Riedl, R. Valentí, and S. M. Winter, Nat. Commun. **10**, 2561 (2019).

[35] T. Ami, M. Crawford, R. Harlow, Z. Wang, D. Johnston, Q. Huang, and R. Erwin, Phys. Rev. B **51**, 5994 (1995).

[36] M. Yamashita, S. Sugiura, A. Ueda, S. Dekura, T. Terashima, S. Uji, Y. Sunairi, H. Mori, E. I. Zhilyaeva, S. A. Torunova *et al.*, npj Quantum Mater. **6**, 87 (2021).

[37] K. Dunnett, J.-X. Zhu, N. Spaldin, V. Juričić, and A. V. Balatsky, Phys. Rev. Lett. **122**, 057208 (2019).

[38] N. M. Hassan, K. Thirunavukkuarasu, Z. Lu, D. Smirnov, E. I. Zhilyaeva, S. Torunova, R. N. Lyubovskaya, and N. Drichko, Phys. Rev. B **104**, 245120 (2021).

[39] Y. Shimizu, K. Miyagawa, K. Kanoda, M. Maesato, and G. Saito, Phys. Rev. Lett. **91**, 107001 (2003).

[40] S. Yamashita, Y. Nakazawa, M. Oguni, Y. Oshima, H. Nojiri, Y. Shimizu, K. Miyagawa, and K. Kanoda, Nat. Phys. **4**, 459 (2008).

[41] S. Yamashita, T. Yamamoto, Y. Nakazawa, M. Tamura, and R. Kato, Nat. Commun. **2**, 275 (2011).

[42] F. Pratt, P. Baker, S. Blundell, T. Lancaster, S. Ohira-Kawamura, C. Baines, Y. Shimizu, K. Kanoda, I. Watanabe, and G. Saito, Nature (London) **471**, 612 (2011).

[43] T. Isono, H. Kamo, A. Ueda, K. Takahashi, M. Kimata, H. Tajima, S. Tsuchiya, T. Terashima, S. Uji, and H. Mori, Phys. Rev. Lett. **112**, 177201 (2014).

[44] Y. Nakamura, N. Yoneyama, T. Sasaki, T. Tohyama, A. Nakamura, and H. Kishida, J. Phys. Soc. Jpn. **83**, 074708 (2014).

[45] Y. Nakamura, T. Hiramatsu, Y. Yoshida, G. Saito, and H. Kishida, J. Phys. Soc. Jpn. **86**, 014710 (2017).

[46] Y. Nakamura, R. Kato, and H. Kishida, J. Phys. Soc. Jpn. **84**, 044715 (2015).

[47] N. Perkins and W. Brenig, Phys. Rev. B **77**, 174412 (2008).

[48] F. Vernay, T. Devereaux, and M. Gingras, J. Phys.: Condens. Matter **19**, 145243 (2007).

[49] M. Holt, B. J. Powell, and J. Merino, Phys. Rev. B **89**, 174415 (2014).

[50] N. Hassan, S. Cunningham, E. I. Zhilyaeva, S. A. Torunova, R. N. Lyubovskaya, J. A. Schlueter, and N. Drichko, Crystals **8**, 233 (2018).

[51] K. Sedlmeier, S. Elsässer, D. Neubauer, R. Beyer, D. Wu, T. Ivek, S. Tomić, J. A. Schlueter, and M. Dressel, Phys. Rev. B **86**, 245103 (2012).